EXPERIMENTAL AND NUMERICAL INVESTIGATION OF FLAME CHARACTERISTICS DURING SWIRL BURNER OPERATION UNDER CONVENTIONAL AND OXY-FUEL CONDITIONS

by

Rastko D. JOVANOVIĆ[a*], Krzysztof STRUG[b], Bartosz SWIATKOWSKI[b], Slawomir KAKIETEK[b], Krzysztof JAGIELLO[b], and Dejan B. CVETINOVIĆ[a]

[a] Laboratory for Thermal Engineering and Energy, Vinca Institute of Nuclear Sciences, University of Belgrade, Belgrade, Serbia

[b] Department of Thermal Processes, Institute of Power Engineering, Warsaw, Poland

Original scientific paper
https://doi.org/10.2298/TSCI161110325J

Oxy-fuel coal combustion, together with carbon capture and storage or utilization, is a set of technologies allowing to burn coal without emitting globe warming CO_2. As it is expected that oxy-fuel combustion may be used for a retrofit of existing boilers, development of a novel oxy-burners is very important step. It is expected that these burners will be able to sustain stable flame in oxy-fuel conditions, but also, for start-up and emergency reasons, in conventional, air conditions. The most cost effective way of achieving dual-mode boilers is to introduce dual-mode burners. Numerical simulations allow investigation of new designs and technologies at a relatively low cost, but for the results to be trustworthy they need to be validated. This paper proposes a workflow for design, modeling, and validation of dual-mode burners by combining experimental investigation and numerical simulations. Experiments are performed with semi-industrial scale burners in 0.5 MW_t test facility for flame investigation. Novel CFD model based on ANSYS FLUENT solver, with special consideration of coal combustion process, especially regarding devolatilization, ignition, gaseous and surface reactions, NO_x formation, and radiation was suggested. The main model feature is its ability to simulate pulverized coal combustion under different combusting atmospheres, and thus is suitable for both air and oxy-fuel combustion simulations. Using the proposed methodology two designs of pulverized coal burners have been investigated both experimentally and numerically giving consistent results. The improved burner design proved to be a more flexible device, achieving stable ignition and combustion during both combustion regimes: conventional in air and oxy-fuel in a mixture of O_2 and CO_2 (representing dry recycled flue gas with high CO_2 content). The proposed framework is expected to be of use for further improvement of multi-mode pulverized fuel swirl burners but can be also used for independent designs evaluation.

Key words: *pulverized coal, swirl burners, oxy-fuel, dual-mode burner stability, CFD modeling*

Introduction

The CO_2, contributes to almost 75% of total GHG emitted to atmosphere [1]. Approximately 35% of emitted CO_2 is produced in fossil-fuel (mainly coal) power plants [2]. As coal

* Corresponding author, e-mail: virrast@vinca.rs

is often the least expensive and locally available energy resource its usage is not expected to decrease, so new low CO_2 combustion technologies must be developed and implemented for CO_2 emissions mitigation [3]. Oxy-fuel combustion, among the other available carbon capture and storage (CCS) technologies [4-6] is considered as the most attractive due to the fact that it is suitable for existing utility boilers [7]. Oxy-fuel combustion is technology in which coal is burned in a mixture of O_2 and recycled flue gas, producing flue gas with a high content of CO_2 ready for segregation [3, 7].

It is important to note that shifting from conventional air combustion to oxy-fuel combustion causes significant difference in all phases of coal combustion process [8-11]. Nearly 1.6 times greater CO_2 specific heat capacity compared with N_2 requires higher O_2 content in the oxidant in case of oxy-fuel combustion in order to obtain similar adiabatic flame temperature as in case of conventional combustion [12]. Higher O_2 concentration in oxidant combined with higher CO_2 density lowers total volumetric flow rate through burner. Since primary oxidant velocities are kept same to keep coal particles in suspension, mass flow rate of primary oxidant is increased during oxy-fuel combustion. This means that total mass flow balance between primary and secondary oxidant streams is changed, and that secondary oxidant mass flow is reduced in oxy-fuel mode. This leads to decrease of secondary oxidant velocity and overall burner swirl level [12]. Summarizing, burner retrofit from conventional to oxy-fuel combustion changes burner aerodynamics and in this way influences flame characteristics (flame ignition position from the burner front, flame length, flame shape).

The CFD is well proven tool for pulverized fuels combustion modeling ranging from experimental furnaces to real scale boilers [13]. The main strength of CFD based models is their capability to give insight into combustion behavior of real scale of interest. Complex and often expensive process of scale-up of laboratory and semi industrial data can be avoided in this way [13]. The CFD tools in recent years are used in development and analysis of new combustion technologies such as oxy-fuel combustion and are also utilized for oxy-fuel burners design [2, 14-16].

Chui *et al.* [17] performed CFD simulations of swirl stabilized 0.3 MW_t burners. Numerical results showed reasonable agreement with experimental data. Toporov *et al.* [18] developed CFD model for oxy-fuel combustion of pulverized coal which was validated against experimental data from oxy-coal swirl burner. Khare *et al*. [12] used CFD modeling to compare ignition mechanisms of an air and an oxy-fuel pulverized coal flames from swirl burners. Bhuiyan and Naser [19] published CFD modeling study of pulverized coal oxy-fuel combustion using International Flame Research Foundation (IFRF) aerodynamically air staged burner. The calculated and experimentally measured values of surface incident radiation were in a satisfying agreement. Vega [20] with coauthors evaluated behavior of bench-scale oxy-burner firing pulverized coal using CFD modeling. Based on numerically optimized values of these parameters new burner concepts which would improve coal particles ignition and ensure stable combustion were suggested.

The main aim of this work is to investigate possibility of existing and improved swirl burner concepts for stable operation during conventional and oxy-fuel combustion. The main focus was on possibility of burner's operation with similar (or ideally same) distribution of flame temperature during both combustion modes which is of great importance for oxy-fuel burner's implementation on existing thermal boilers [15]. However, the presented study focuses not only on stable burner operation, but also offers deeper insight in pulverized coal swirl flame differences during transition from air to oxy-fuel combustion. Necessity for improved burner design is drawn based on conclusions from firing pulverized coal in conventional and

oxy-fuel modes using existing swirl burner. Furthermore, this study suggests new swirl burner design based on geometrical modification of existing burner concept. The novel oxy-coal burner performance is investigated next. This study, in its final phase, aims to confirm new burner concept's ability for a stable performance in both conventional and oxy-fuel combustion regimes, concentrating on flame aerodynamics, stable ignition, similar temperature distribution inside combustion furnace, and pollutant emissions during both combustion regimes. Utilized investigation methodology is shown in fig. 1

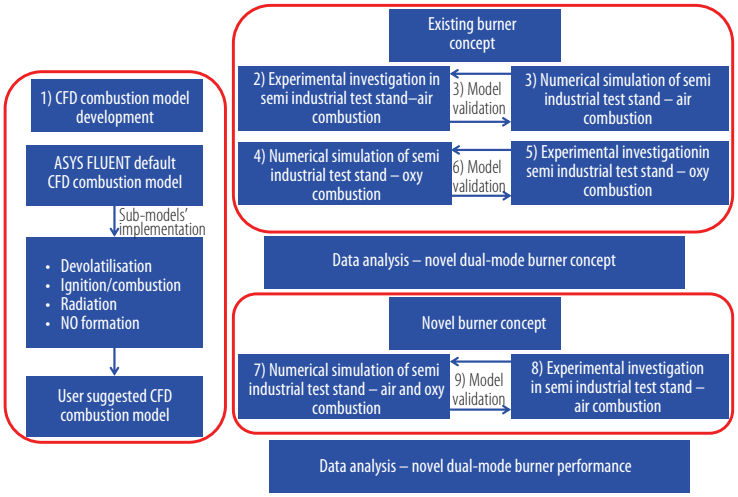

Figure 1. Pulverized burners investigation and design methodology

Experimental facility

All experiments were performed on 0.5 MW_t semi-industrial stand. The experimental stand is equipped with system for flue gas re-circulation, but it can also be used in a once-through operating mode, fig. 2. The main elements of test facility are: 1 – burner prototype, 2 – cylindrical furnace with inner diameter of 700 mm and total length of 7000 mm, 3 – coal mill, 4 – coal bunker, 5 – collector for O_2/CO_2 mixture generation, 6 – duct used in a once-through mode for primary oxidant transport, 7 – primary oxidant heater, 8 – heavy oil supply for the furnace start-up and flame support, 9 – duct used in a once-through mode for secondary oxidant transport, 10 – secondary oxidant pre-heater, 11 – heavy oil storage for secondary oxidant pre-heaters, 13 – secondary oxidant electrical heaters. The test furnace is equipped with a system observation, flame recording, in-flame temperature measurements, and gas sampling and analysis – 14, 15. Series of heat exchangers were built-in for cooling furnace walls – 16. Flue gas exiting furnace passes through the cyclone separators – 17 and then is introduced into the chimney – 18. When the experimental facility works in a wet flue gas re-circulation mode, flue gas re-circulation system – 12 is used to recycle desired flue gas portion back to the secondary oxidant ducts – 9, where it is mixed with a pure O_2 (99.995%) from O_2 tanks introduced through the duct – 19.

All experiments under oxy-fuel conditions in the presented work were performed in once-through mode, similarly to [21], which is easier for control, and more flexible to change of working parameters (mass flows, re-circulation ratios). Recycled flue gas was represented with a CO_2, while desired oxidant composition is obtained mixing O_2 and CO_2. Only dry recalculation cases were evaluated in this study. Re-circulation ratio (*RR*) is defined:

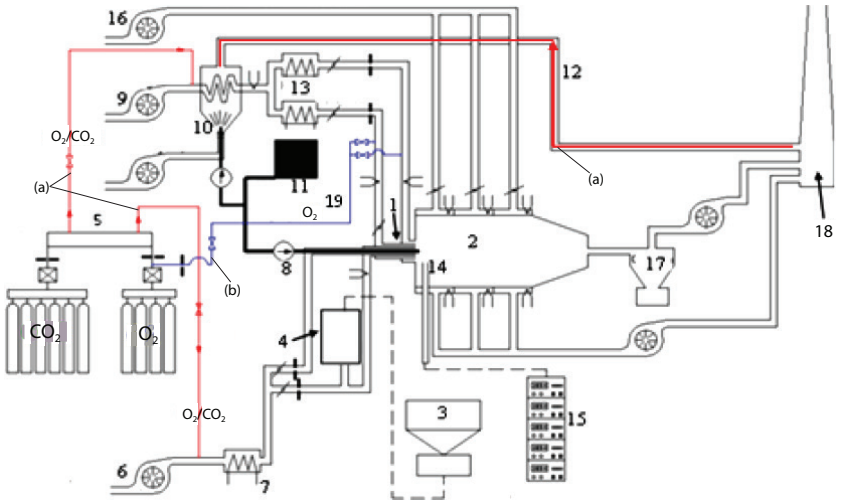

Figure 2. Schematic representation of semi-industrial test facility, red (a) and blue (b) lines represent retrofitted elements for oxy-fuel experiments
(*for color image see journal web site*)

$$RR = \frac{\dot{m}_{RFG}}{\dot{m}_{RFG} + \dot{m}_{PFG}} \tag{1}$$

where $\dot{m}_{RFG}$ and $\dot{m}_{PFG}$ are recycled gas and product gas mass flow rates, respectively. Experimental facility is able to work in wide range of *RR* values (up to 85%). In order to compare two different burner concepts *RR* values should ideally be kept the same or at least similar. The existing and novel burner performance was evaluated for *RR* = 0.77 and for *RR* = 0.79, respectively. These *RR* values were chosen in order to obtain similar adiabatic flame temperature during air and oxy-fuel coal combustion.

Table 1(a). Coal chemical properties

Coal chemical analysis lower heating value (LHV), and higher heating value (HHV)						
Proximate analysis (as received)					Heating value	
Quantity	Moisture	Volatiles	Fixed carbon	Ash	LHV	HHV
Unit	[%]	[%]	[%]	[%]	[kJkg^{-1}]	[kJkg^{-1}]
Value	4.0	23.5	59.5	13	26582	27528
Ultimate analysis (as received)						
C [%]	H [%]	O [%]	N [%]	S [%]		
69.83	3.86	7.04	1.64	0.61		

Table 1(b). Particle size distribution

Fuel	Diameter, d [μm]	Mass fraction $Y > d$ [%]
South African coal	200	3.078
	125	15.86
	90	29.66
	63	49.41
	32	87.06

Experimental procedure

South African bituminous coal was used in all experiments. Coal characteristics are shown in tab. 1(a). Coal was pulverized using MKM-25 ball-ring mill to five portions of polydispersed dust. Measured coal size distribution, shown in tab. 1(b), was fitted to the Rosin-Rammler distribution with the following parameters: $d_{P,\min}$ = 1e–05 m, $d_{P,\max}$ = 2e–04 m, $d_{P,\text{mean}}$ = 6.5e–05 m, spread factor = 1.15. Gas temperature was measured using S-type PtRh/Pt thermocouple mounted on stainless steel rod. Thermocouple is placed within ceramic tip and in this way shielded form radiation influence.

Main burner operating parameters are shown in tab. 2. Maximal temperature measuring uncertainty, calculated according to EN 60584-2 standard, is ±5 ºC. Temperature values at different axial distances from burner front and NO and CO values at the furnace outlet were measured during experimental campaign. These values were monitored and measured during each test. Average experimental test lasted about 30 minutes. Each successful test was repeated on two different days. Gas temperature was measured at five different radial positions at three different measuring axes. Measuring axes were positioned at distances of 180 mm, 440 mm, and 1300 mm from the investigated burner front. Average temperature values presented in this work are calculated for each measuring axis as a mean of all measured values from all five radial positions. Flue gases composition was measured by set of Siemens Ultramat 23 and FUJY ZKJ3 analyzers. The CO and NO content in the flue gas were determined with measuring uncertainty of ±12% and ±5% of the measured value, respectively. The measuring uncertainty budgets comprise contribution from calibration gas uncertainty, linearity, repeatability, zero and span drift and relevant influence quantity.

Different burner geometries investigated in this study are shown in fig. 3. The main difference between two burner geometries is that while in the existing burner concept secondary oxidant is introduced through the single duct (secondary oxidant annulus), fig. 3(a), in case of novel burner concept it is introduced through the two separate ducts (inner and outer), fig. 3(b). Mass flow rates through these two secondary oxidant ducts can be controlled using special movable shutter. Novel burner concept is designed in that way that during air combustion stable performance is achieved introducing secondary oxidant only through the outer secondary annulus while during oxy-fuel combustion movable shutter is used to redirect desired secondary oxidant portion from the outer secondary annulus toward the inner secondary annulus to obtain similar momentum ratio to those during air combustion, and thus enabling stable operation in the both combustion modes.

Table 2. Main operating parameters during coal combustion investigation

Quantity	Existing burner concept		Novel burner concept		
	Conventional combustion	Oxy combustion	Conventional combustion	Oxy combustion	
Pulverized coal mass flow rate [kgh^{-1}]	50.6	50.6	50.6	50.6	
Primary oxidant mass flow rate [kgh^{-1}]	92.09	131.55	63.92	91.28	
Secondary oxidant mass flow rate [kgh^{-1}]	220.47	181.01	315.37	Inner annulus	158.41
				Outer annulus	129.61
Primary oxidant temperature [K]	373	373	373	373	
Secondary oxidant temperature [K]	553	553	553	553	
Primary oxidant composition (molar basis)	21% O_2, 79% N_2	22% O_2, 78% CO_2	21% O_2, 79% N_2	22% O_2, 78% CO_2	
Secondary oxidant composition (molar basis)	21% O_2, 79% N_2	35% O_2, 65% CO_2	21% O_2, 79% N_2	35% O_2, 65% CO_2	
Secondary oxidant swirl angle [º]	50	50	50	50	

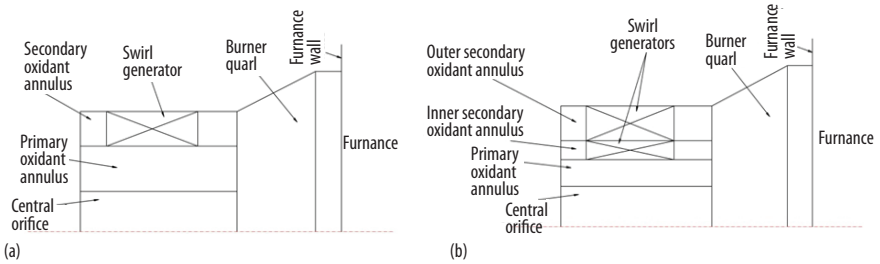

Figure 3. Investigated burner geometries; (a) existing concept and (b) novel concept

The CFD model

The main model features are described in the following text. The CFD model is based on comprehensive CFD code ANSYS FLUENT 13. Axisymmetric swirl solver was chosen since it provides good accuracy with relatively low computational demand [22]. Moreover, it is widely used in scientific community for pulverized fuel swirl burners CFD modeling both in air and in oxy-fuel conditions [18, 23-25]. Solver choice was additionally justified by the symmetrical geometry and an expected flow field symmetry [26, 27]. The following fluid flow characteristics were assumed: incompressible, ideal gas, multi-component flow. Mixture specific heat, viscosity, and thermal conductivity were determined based on ideal gas mixing law. Temperature dependent values for specific heat, viscosity and thermal conductivity of individual species in 4th order polynomial form were taken from FLUENT fluid materials database (which is based on CHEMKIN materials data library) [22]. Reactive gaseous multicomponent turbulent flow was solved using Eulerian approach. Realizable κ-ε [28] turbulence model was used for turbulence modeling due to its ability to more accurately predict turbulent jet spreading and re-circulation zones, compared with standard κ-ε turbulence model [29]. Standard wall functions [22] were employed as turbulence boundary condition at computational domain wall cells [30].

Secondary phase (pulverized coal particles) was solved in Lagrangian reference frame. Particle trajectory is computed by integrating the force balance acting on the each computational particle. Influence of drag force and gravity force was modeled. Influence of secondary phase properties on fluid flow is taken into account using appropriate source terms in Eulerian equations. Source terms interphase exchange is set to occur at every twenty primary phase iterations.

The discrete ordinates (DO) model [31] was used to solve radiation transfer equation. The DO model equation was solved using equal quadrature divisions in four directions (4 × 4). WSGG model was used to calculate gas emissivity with a novel set of model coefficients, [32], applicable for both air and for oxy-fuel combustion, implemented as user defined function (UDF). The emissivity for all wall surfaces was set to 0.8. Particle absorption and scattering coefficients were set to 0.8 1/m and 0.3 1/m, respectively [13].

Devolatilization modeling

The main shortcomings of default FLUENT devolatilization models are the following: volatiles are represented by a single generic HC, and devolatilization rate is defined by the set of Arrhenius constants which have to be experimentally determined for each fuel sample in order to properly describe devolatilization. In order to overcome these shortcomings, more advanced, general network functional group (FG) devolatilization model was implemented in FLUENT solver using UDF.

The FG model represents coal particle structure as a network composed of aromatic clusters connected with different FG which are broken during devolatilization and released as light gaseous species. Tar evolution is represented as a parallel process which competes for FG. Use of coal independent rates of individual FG is important feature of FG model. Namely, model only needs coal proximate and ultimate analysis as an input, and does not require determination of Arrhenius kinetic constants [25, 33].

Initial volatile fractions of each species in coal particle were determined using correlations proposed in work of Merrick [34]. Following the proposed correlations, mass fractions of carbon char, main gaseous species: CH_4, C_2H_6, CO, CO_2, H_2, H_2O, NH_3, H_2S, and tar were determined. Initial mass fractions partition for main volatile N species was adopted according to recommendation for bituminous coals, $HCN/NH_3 = 9/1$ [35].

Chemical reaction modeling

Gaseous reactions were modeled using finite-rate/eddy dissipation model which predicts that reaction rate is controlled by the slower of the two processes: species turbulent mixing rate and chemical kinetics. Semi-global chemical reaction mechanism is composed of totally five global reactions in gaseous phase $r_G(i)$, as shown in tab. 3. Reaction mechanism is modified for oxy-fuel combustion conditions and its accuracy is widely established with comparison with different theoretical calculations and experimental data [38-40].

Surface reactions were modeled using the kinetics/diffusion-limited rate model which is based on reaction chemical kinetics rate and the external diffusion rate of reactant to the char surface. Diffusion rate is determined using diffusion rate coefficient which is function of: particle temperature, gas phase temperature, and diffusion rate constant, C_j. Surface reaction kinetic mechanism, built in as UDF is composed of totally three different char surface reactions (r_c) as shown in tab. 4.

Ignition modeling

Default FLUENT ignition/combustion model is able to predict only homogeneous ignition of completely devolatilized coal particle [22]. User developed ignition/combustion

Table 3. Gaseous reactions kinetic data

Reaction	Reaction expression	Reaction kinetics expression	A_j [kmol m^{-3}s^{-1}]	$E_{a,j}$ [Jkmol^{-1}]	Ref.
$r_G(1)$	$CH_4 + 0.5O_2 \rightarrow CO + 2H_2$	$\frac{d[CH_4]}{dt} = A_j e^{-\frac{E_{a,j}}{RT_G}} [CH_4]^{0.5} [O_2]^{1.25}$	4.4e+11	1.26e+08	[36]
$r_G(2)$	$CH_4 + H_2O \rightarrow CO + 3H_2$	$\frac{d[CH_4]}{dt} = A_j e^{-\frac{E_{a,j}}{RT_G}} [CH_4]^{1} [O_2]^{1}$	3.0e+08	1.26e+08	[36]
$r_G(3)$	$tar(C_uH_v) + 0.5uO_2 \rightarrow uCO + 0.5vH_2$	$\frac{d[tar]}{dt} = A_j e^{-\frac{E_{a,j}}{RT_G}} [tar]^{1} [O_2]^{1}$	3.8e+07	5.55e+07	[37]
$r_G(4)$	$H_2 + 0.5O_2 \rightarrow H_2O$	$\frac{d[H_2]}{dt} = A_j e^{-\frac{E_{a,j}}{RT_G}} [H_2]^{1} [O_2]^{0.5}$	5.69e+11	1.465e+08	[36]
$r_G(5)$	$CO + 0.5O_2 \rightarrow CO_2$	$\frac{d[CO]}{dt} = A_j e^{-\frac{E_{a,j}}{RT_G}} [CO]^{1} [O_2]^{0.25} [H_2O]^{0.5}$	2.24e+06	4.18e+07	[36]

Table 4. Surface reactions kinetic constants and diffusion coefficients

Reaction	Reaction expression	A_j [kgm^{-2}s^{-1}Pa^{-1}]	$E_{a,j}$ [Jkmol^{-1}]	Temperature range [K]	Ref.	C_j^a [s(K$^{0.75}$)$^{-1}$]	C_j^b [s(K$^{0.75}$)$^{-1}$]	Ref.
$r_c(1)$	C(*s*) + 0.5O$_2$ → 2CO	0.005	7.4e+07	Whole range	[18]	5.32e–12	4.13e–12	[7]
$r_c(2)$	C(*s*) + H$_2$O → CO + H$_2$	0.319 0.00192	2.08e+08 1.47e+08	<1273 ≥1273	[18]	5.77e–12	4.12e–12	
$r_c(3)$	C(*s*) + CO$_2$ → 2CO	0.000135 0.00635	1.355e+08 1.62e+08	<1223 ≥1223	[18]	1.72e–12	1.69e–12	

(a) During conventional combustion, (b) during oxy-fuel combustion

mechanism takes into account both homogeneous ignition/combustion of totally devolatilized coal particle and heterogeneous ignition/combustion of non-devolatilized or partially devolatilized coal particle. The proposed user model assumes that necessary condition for heterogeneous non-devolatilized or partially devolatilized coal particle ignition is that mass loss due to coal particle oxidation is higher than mass loss due to devolatilization:

$$r_{\text{coal}} \geq \sum_i r_{\text{devol},i} \tag{2}$$

Kinetics/diffusion-limited rate model was used both for coal reaction and for char reactions. However, different Arrhenius parameters (compared with char reaction $r_c(1)$) were used for coal combustion reaction: $A_{\text{coal}} = 0.86$ kg/(m^2·s·Pa) and $E_{a,\text{coal}} = 1.49\text{e+}08$ J/kmol [41]. Condition (2) was implemented in FLUENT code as UDF which is checked for each particle at the beginning of each discrete time step Δt. If condition (2) is met for the considered computational particle in discrete time step, Δt, particle mass loss of that particular computational particle occurs both due to devolatilization and due to char combustion which corresponds to heterogeneous particle ignition/combustion mechanism. However, if condition (2) is not satisfied it is assumed that homogeneous ignition takes place. In this case model assumes that while there are remaining volatiles inside particle mass loss of considered computational particle is caused only by devolatilization process, which simulates burning particle surrounded by combusting volatile flame. Then, when all volatiles are released, char combustion takes place, and mass loss of considered computational particle comes only from char reactions.

The NO formation modeling

The NO transport equations were solved as a post-processing step, decoupled of previously calculated flow field. It was assumed that NO is formed via two main mechanisms: thermal NO formed by oxidation of N_2 present in oxidant and fuel NO formed by oxidation of N_2 bound inside coal particles. It was assumed that char N_2 is directly released in NO. Volatile NO formation was represented as two-step process. The N_2 which evolves from coal during devolatilization stage forms NH_3 and HCN as intermediate species which are than oxidized and reduced by a set of competitive reactions to form NO and N_2. The NO formation scheme is shown in fig. 4. N_2 partition between char and volatiles is very important during NO formation, as reported in [16]. Furthermore, initial HCN/NH_3 ratio also has significant influence on final fuel NO formation. Widely used approach is to assume that N_2 is split between fuel and char proportionally to coal experimental analysis, while HCN/NH_3 ratio is commonly adopted based on experimental or modeling experiences for different coal ranks [5]. In the presented investigation N_2 split between fuel and char and HCN/NH_3 ratio are obtained directly from FG devolatilization model. Reaction kinetics $k_1 - k_4$ is represented by well-known De Soete [42] mechanism.

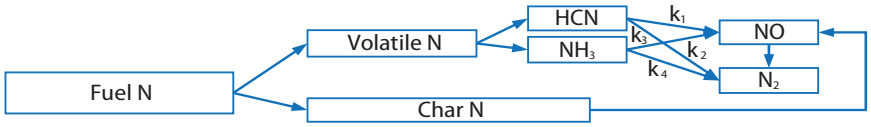

Figure 4. The NO formation scheme

Results and discussion

Grid generation and grid independence study

Grid independence study was performed gradually increasing cell number in the near burner zone. Four different meshes, consisting of 66289, 142000, 216600, and 343000 cells, respectively, were constructed to check grid independence, fig. 5(a) and 5(b). Air combustion simulation using existing burner was used to establish grid independent solution. Averaged values of static temperature in vertical cross-sections obtained for different mesh finesses are presented in fig. 5(c). Computational mesh consisting of 216600 control volumes was adopted for further CFD simulations.

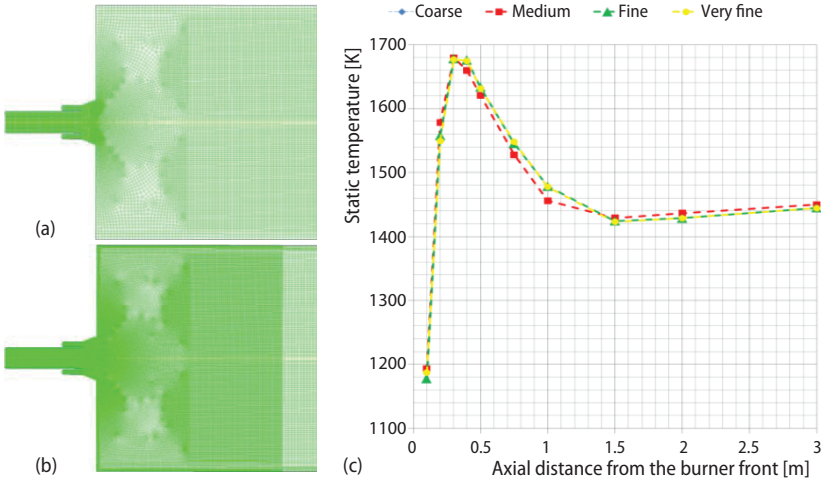

Figure 5. (a) Initial computational mesh, (b) adopted refined computational mesh, and (c) grid independence test results, averaged static temperature values at different axial distances
(*for color image see journal web site*)

Analysis of air and oxy-fuel combustion performance using existing burner concept

Primary oxidant velocity was kept same for both combustion modes in order to keep pulverized coal particles in suspension. Mass flow rate of primary oxidant is thus increased switching to oxy-fuel combustion mode. Consequently, recycled flue gas mass flow fed to secondary oxidant is decreased and because of this secondary oxidant velocity during oxy-fuel combustion is lowered.

The CFD simulations showed that type-2 flame (by IFRF classification [43]) is developed during conventional combustion. Flame is characterized by the presence of the closed inner re-circulation zone, fig. 6(a). This is short, intense, stable flame ignited close to the burner

front, fig. 7(a). Described changes in flow rates significantly affect burner aerodynamics and during oxy-fuel combustion lead to flame type change, from type-2 to type-1 flame. Type-1 is flame characterized by penetration of the primary oxidant-fuel stream through the inner recirculation zone, and by the separation of this zone into two new inner recirculation zones, fig. 6(b). Described flame aerodynamics causes delayed ignition further from the burner front and increase in flame length, fig. 7(b). The flame shape is also affected by the central oil gun, which acts as a bluff-body and causes additional small inner recirculation, fig. 6.

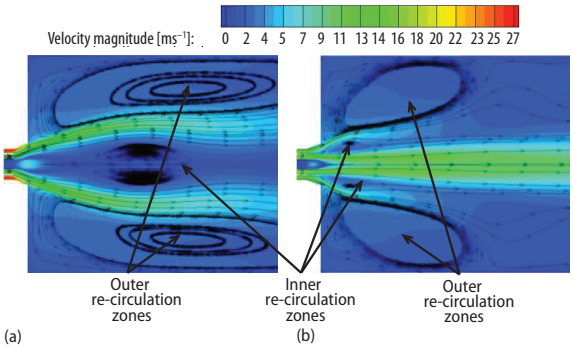

Figure 6. Near burner zone flow field, existing burner: (a) air combustion, (b) oxy-fuel combustion
(*for color image see journal web site*)

Comparison between CFD obtained and measured temperatures at different axial distances from the burner front, and CO and NO values at furnace outlet is shown in fig. 8. It can be seen that modeled and experimental values are in satisfying agreement. Somewhat lower numerically calculated temperature values compared with an experimentally determined, with a relative difference up to about 9%, can be contributed to a thermocouple ceramic shielding, which probably did not completely protect thermocouple junction from radiation influence. Importantly, although similar values of maximal temperatures were obtained during both air and oxy-fuel combustion, fig. 8(a), it can be seen that temperature distribution in near burner zone significantly differs between these two combustion technologies, figs. 7 and 8(a). Bigger temperature values present in near burner zone during air combustion compared with oxy-fuel combustion additionally confirm delayed ignition in the former case, which may influence combustion performance. This conclusion is confirmed by predicted and measured CO and NO values, fig. 8(b). The CO fraction in flue gas increases when switching from air to oxy-fuel combustion which can be consequence of decreased inner re-circulation zone and higher velocity values in axial direction which decrease particle residence time and lower char burnout. The NO values are somewhat lower in case of oxy-fuel than in case of air combustion. This NO reduction during oxy-fuel combustion is a result of thermal NO suppression caused by absence of air N_2.

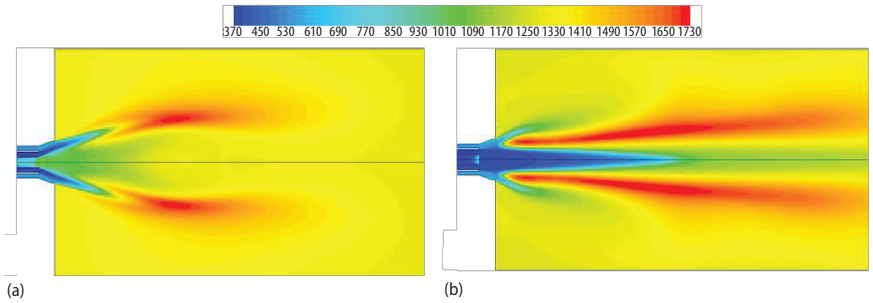

Figure 7. Flame shape inside furnace, existing burner; (a) air combustion, (b) oxy-fuel combustion
(*for color image see journal web site*)

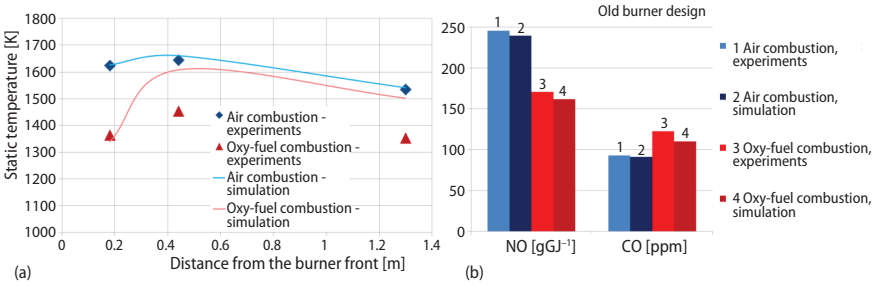

Figure 8. (a) Static temperature values at different axial distances from burner front, (b) CO and NO values at the furnace outlet – improved burner concept
(*for color image see journal web site*)

Analysis of air and oxy-fuel combustion performance using improved burner concept

Decrease of combustion performance when switching from air combustion to oxy-fuel combustion described in the previous paragraph was mainly caused by flame aerodynamics changes. Momentum ratio, defined as the ratio of primary to secondary momentum flux:

$$R_M = \frac{\vec{V}_{prim}\,\dot{m}_{prim}}{\vec{V}_{sec}\,\dot{m}_{sec}}$$

may be used to characterize influence of primary and secondary flows on flame aerodynamics [12, 44]. Momentum ratio increased from 0.18 in case of air combustion to 0.53 in case of oxy-fuel combustion using existing burner concept which shows dominant effect of the primary flow in determining the flame aerodynamics.

Based on this, it was decided to design and develop improved burner concept which would maintain similar (or ideally same) flame aerodynamics and temperature distribution during both combustion modes. Stable burner operation during both combustion modes is essential for dual-burners design which has to enable stable burner performance in air mode during boiler start-up (and in emergency situations) and in oxy-fuel mode during boiler operation. This was achieved dividing secondary oxidant flow into two separate annulus-shaped ducts, fig. 3. Approximately about 75% of total available secondary oxidant mass was injected through the inner secondary annulus which enabled to obtain momentum ratio value during oxy-fuel combustion (0.114) close to that during air combustion (0.106). The CFD simulation based results showed that similar values of momentum ratio during different combustion technologies (air and oxy-fuel) have positive impact on flame aerodynamics. Namely, type-2 flame is developed during both air and oxy-fuel combustion as can be seen in fig. 9. Similar flame aerodynamics resulted in similar temperature distribution in near burner zone, fig. 10.

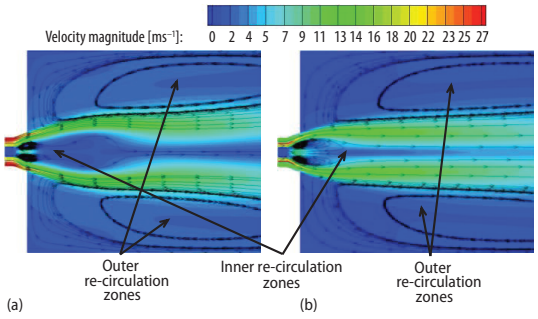

Figure 9. Near burner zone flow field, novel burner; (a) air combustion, (b) oxy-fuel combustion
(*for color image see journal web site*)

Based on these results improved burner design was produced and was used for experimental investigations of combustion performance and for CFD model accuracy verification. Experimentally measured and numerically obtained static temperature values at different axial distances and CO and NO values at furnace outlet are shown in fig. 11.

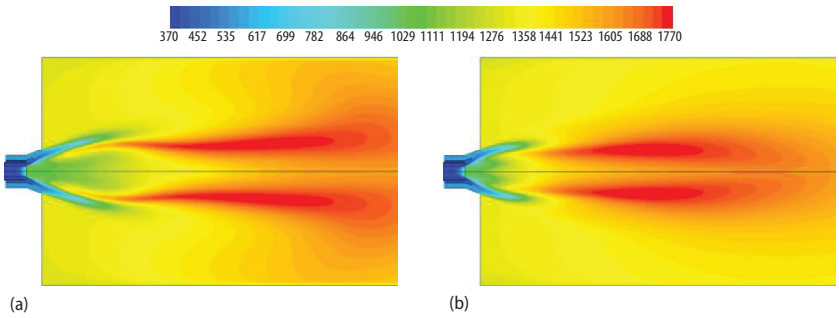

Figure 10. Flame shape inside furnace, novel burner: (a) air combustion, (b) oxy-fuel combustion
(*for color image see journal web site*)

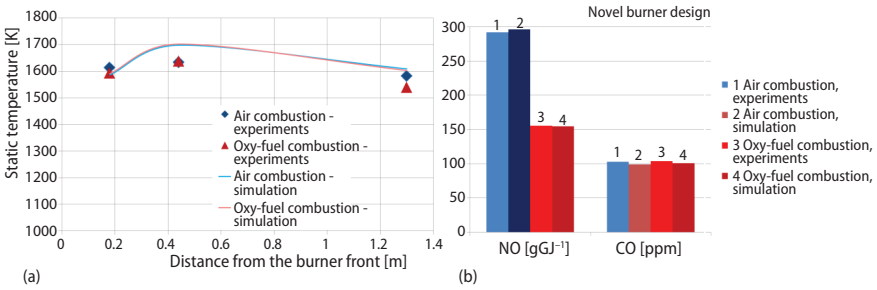

Figure 11. (a) Static temperature values at different axial distances from burner front, (b) CO and NO values at the furnace outlet – improved burner concept
(*for color image see journal web site*)

It can be seen that CFD and experimental results are in satisfying agreement. It is important to underline close values of static temperature at different axial distances from burner front during both air and oxy-fuel combustion using improved burner design. This shows ability of the newly designed burner for a stable performance in both investigated combustion modes. Improvement in burner performance can be observed in CO emission at burner outlet when switching from air to oxy-fuel combustion mode. While CO emission was higher during oxy-fuel combustion using old burner design, fig. 8(b), there is no CO emission increase switching from air to oxy-fuel combustion using improved burner, fig. 11(b), which additionally confirms good combustion performance of newly designed burner for both air and oxy-fuel combustion technologies. The NO reduction during oxy-fuel combustion is more noticeable in case of improved burner compared with existing burner, figs. 8(b) and 11(b). This can be contributed to combined effects of absence of thermal NO and improved flame characteristics during oxy-fuel combustion using newly designed burner concept. Type-2 flame which is also developed during oxy-fuel combustion with new burner is characterized with the presence of closed internal O_2 lean recirculation zone which favors fuel NO reduction [45].

Conclusions and future work

Novel concept of burner development which combines experimental investigation and advanced CFD simulations in the single framework was suggested. As the CFD and experimental data confirmed lower burner performance during oxy-fuel combustion due to change in flame aerodynamics it was decided to design novel burner concept able to operate with satisfying performance in both combustion modes. Improved burner performance was checked using CFD simulation. The obtained results confirmed that, as expected, during both air and oxy-fuel combustion stable flame with similar aerodynamics (type-2 flame) and similar temperature distribution inside furnace would be obtained. Conclusions obtained from numerical simulations were experimentally proven on novel burner prototype. Very close agreement between CFD calculated and experimentally measured values proved model ability for pulverized coal oxy-fuel combustion simulation. Significant decrease in NO emissions was achieved during oxy-fuel combustion, while there was no increase in CO emissions, using novel burner concept, compared with air combustion. Novel burner concept, designed in Institute for Power Engineering, Warsaw, Poland, is of paramount importance, as it can be used for real scale boiler retrofit to oxy-fuel combustion technology without additional changes in boiler equipment. The established burner investigation and development methodology leaves broad range of operating parameters, which influence on burner performance will be subject of further work. Parameters include, but are not necessarily limited to: fuel type, grinding and resulting PSD, flue gas recirculation ratio, swirl angle. The performed work demonstrated that suggested methodology can be successfully applied in further improvement in burner design or for new burner concepts development.

Acknowledgment

The authors would like to acknowledge high appreciation for the support and promotion of this work to the Public Enterprise *Electric power industry of Serbia*, Belgrade, Serbia, and Ministry of Education and Science of Republic of Serbia (Project No. III42010 and TR33050). Experimental study was funded by the European Commission 6th FP through the Marie Curie Actions project INECSE (Early Stage Research Training in Integrated Energy Conversion for a Sustainable Environment), EU-CONTRACT-NUMBER: MEST-CT-2005-021018.

Nomenclature

A – pre-exponential factor (units vary)
C – average molar concentration of the gaseous species, [kmol m^{-3}]
d – diameter, [m]
E_a – activation energy, [J kmol^{-1}]
k – kinetic or diffusion rate, [kg m^{-2} s^{-1} Pa^{-1}]
$\dot{m}$ – mass flow rate, [kg s^{-1}]
MW – molecular weight, [kg kmol^{-1}]
R – gas constant (= 8.314), [J kmol^{-1}K^{-1})]
R_M – momentum ratio, [–]
RR – recycle ratio, [–]
r – reaction (process) rate, [kg s^{-1}]
S – surface area, [m^2]
Y – mass fraction, [–]

Greek symbols

ε/k – large-eddy mixing scale, [s^{-1}]
v – stoichiometric coefficient, [–]

Subscripts

devol – devolatilization
G – gaseous phase
i – component number
j – chemical bond or chemical reaction number
P – particle
PFG – product fuel gas
pf – pulverized fuel (coal)
$prim$ – primary burner stream
RFG – recycled fuel gas
sec – secondary burner stream

Acronyms

DO – discrete ordinates
FG – functional group
HHV – higher heating value
LHV – lower heating value
UDF – user defined function

References

[1] ***, Information on Global Warming Potentials, Technical paper, Report No. FCCC/TP/2004/3, United Nations, New York, USA, 2004
[2] Edge, P. J., *et al.,* A Reduced Order Full Plant Model for Oxyfuel Combustion, *Fuel*, *101* (2012), 1, pp. 234-243
[3] Wall, T., *et al.,* An Overview on Oxyfuel Coal Combustion – State of the Art Research and Technology Development, *Chemical Engineering Research and Design*, *87* (2009), 8, pp. 1003-1016
[4] Vorrias, I., *et al.,* Calcium Looping for CO_2 Capture from a Lignite Fired Power Plant, *Fuel*, *113* (2013), 1, pp. 826-836
[5] Nikolopoulos, N., *et al.,* Numerical Investigation of the Oxy-Fuel Combustion in Large Scale Boilers Adopting the ECO-Scrub Technology, *Fuel*, *90* (2011), 1, pp. 198-214
[6] Hossain, M. M., de Lasa, H. I., Chemical-Looping Combustion (CLC) for Inherent Separations – A Rreview, *Chemical Engineering Science*, *63* (2008), 18, pp. 4433-4451
[7] Chen, L., *et al*., Oxy-Fuel Combustion of Pulverized Coal: Characterization, Fundamentals, Stabilization and CFD Modeling, *Progress in Energy and Combustion Science*, *38* (2012), 2, pp. 156-214
[8] Rathnam, R. K., *et al.,* Differences in Reactivity of Pulverised Coal in Air (O_2/N_2) and Oxy-Fuel (O_2/CO_2) Conditions, *Fuel Processing Technology*, *90* (2009), 6, pp. 797-802
[9] Shaddix, C. R., Molina, A., Particle Imaging of Ignition and Devolatilization of Pulverized Coal During Oxy-Fuel Combustion, *Proceedings of the Combustion Institute, 32* (2009), 2, pp. 2091-2098
[10] Qiao, Y., *et al.,* An Investigation of the Causes of the Difference in Coal Particle Ignition Temperature between Combustion in Air and in O_2/CO_2, *Fuel, 89* (2010), 11, pp. 3381-3387
[11] Bejarano, P. A., Levendis, Y. A., Single-Coal-Particle Combustion in O_2/N_2 and O_2/CO_2 Environments, *Combustion and Flame, 153* (2008), 1-2, pp. 270-287
[12] Khare, S. P., *et al.,* Factors Influencing the Ignition of Flames from Air-Fired Swirl PF Burners Retrofitted to Oxy-Fuel, *Fuel, 87* (2008), 7, pp. 1042-1049
[13] Williams, A., *et al.,* Modelling Coal Combustion: the Current Position, *Fuel*, *81* (2002), 5, pp. 605-618
[14] Al-Abbas, A. H., *et al*., CFD Modelling of Air-Fired and Oxy-Fuel Combustion of Lignite in a 100 kW Furnace, *Fuel, 90* (2011), 5, pp. 1778-1795
[15] Al-Abbas, A. H., *et al*., CFD Modelling of Air-Fired and Oxy-Fuel Combustion in a Large-Scale Furnace at Loy Yang a Brown Coal Power Station, *Fuel, 102* (2012), 1, pp. 646-665
[16] Alvarez, L., *et al.,* CFD Modeling of Oxy-Coal Combustion: Prediction of Burnout, Volatile and NO Precursors Release, *Applied Energy, 104* (2013), 1, pp. 653-665
[17] Chui, E. H., *et al*., Modeling of Oxy-Fuel Combustion for a Western Canadian Sub-Bituminous Coal, *Fuel, 82* (2003), 10, pp. 1201-1210
[18] Toporov, D., *et al.,* Detailed Investigation of a Pulverized Fuel Swirl Flame in CO_2/O_2 Atmosphere, *Combustion and Flame*, *155* (2008), 4, pp. 605-618
[19] Bhuiyan, A. A., Naser J., Numerical Modelling of Oxy Fuel Combustion, the Effect of Radiative and Convective Heat Transfer and Burnout, *Fuel, 139* (2015), 1, pp. 268-284.
[20] Vega, F., *et al.,* Geometrical Parameter Evaluation of a 0.5 MWth Bench-Scale Oxy-Combustion Burner, *Fuel, 139* (2015), 1, pp. 637-645
[21] Smart, J., *et al.,* Characterisation of an Oxy-Coal Flame Through Digital Imaging, *Combustion and Flame, 157* (2010), 6, pp. 1132-1139
[22] ***, ANSYS Inc., ANSYS FLUENT 13.0 Theory Guide Rrelease 12.0., 2009
[23] Hu, Y., Yan, J., Numerical Simulation of Radiation Intensity of Oxy-Coal Combustion with Flue Gas Recirculation, *International Journal of Greenhouse Gas Control, 17* (2013), 1, pp. 473-480
[24] Rebola, A., Azevedo, J. L. T., Modelling Coal Combustion with Air and Wet Recycled Flue Gas as Comburent in A 2.5 MW_{th} Furnace, *Applied Thermal Engineering*, *86* (2015), 1, pp. 168-177
[25] Richter, A., *et al*., Detailed Analysis of Reacting Particles in an Entrained-Flow Gasifier, *Fuel Processing Technology*, *144* (2016), 1, pp. 95-108
[26] Jovanovic, R., *et al.,* Sensitivity Analysis of Different Devolatilisation Models on Predicting Ignition Point Position during Pulverized Coal Combustion in O_2/N_2 and O_2/CO_2 Atmospheres, *Fuel, 101* (2012), 1, pp. 23-37

[27] Jovanovic, R., *et al.,* Numerical Investigation of Influence of Homogeneous/Heterogeneous Ignition/Combustion Mechanisms on Ignition Point Position During Pulverized Coal Combustion in Oxygen Enriched and Recycled Flue Gases Atmosphere, *International Journal of Heat and Mass Transfer, 54* (2011), 4, pp. 921-931
[28] Shih, T. H. *et al.,* A New *k-ε* Eddy-Viscosity Model for High Reynolds Number Turbulent Flows – Model Development and Validation, *Computers and Fluids*, *24* (1995), 3, pp. 227-238
[29] Launder, B. E., Spalding, D. B., *Lectures in Mathematical Models of Turbulence*, Academic Press, London, 1972
[30] Launder, B. E., Spalding, D. B., The Numerical Computation of Turbulent Flows, *Computer Methods in Applied Mechanics and Engineering*, *3* (1974), 2, pp. 269-289
[31] Chui, E. H., Raithby, G. D., Computation of Radiant Heat Transfer on a Non-Orthogonal Mesh Using the Finite-Volume Method, *Numerical Heat Transfer, Part B*, *23* (1993), 3, pp. 269-288
[32] Yin, C., *et al.,* New Weighted Sum of Gray Gases Model Applicable to Computational Fluid Dynamics (CFD) Modeling of Oxy-Fuel Combustion: Derivation, Validation, and Implementation, *Energy and Fuels*, *24* (2010), 12, pp. 6275-6282
[33] Solomon, P. R., *et al.,* General Model of Coal Devolatilization, *Energy and Fuels*, *2* (1998), 4, pp. 405-422
[34] Merrick, D., Mathematical Models of the Thermal Decomposition of Coal 1, the Evolution of Volatile Matter, *Fuel*, *62* (1983), 5, pp. 535-539
[35] Glarborg, P., *et al*., Fuel Nitrogen Conversion in Solid Fuel Fired Systems, *Progress in Energy and Combustion Science*, *29* (2003), 2, pp. 89-113
[36] Andersen, J., *et al.,* Global Combustion Mechanisms for Use in CFD Modeling under Oxy-Fuel Conditions, *Energy and Fuels*, *23* (2009), 3, pp. 1379-89
[37] Shaw, D. W., *et al.,* Determination of Global Kinetics of Coal Volatiles Combustion, *Symposium (International) on Combustion*, *23* (1991), 1, pp. 1155-1162
[38] Prieler, R., *et al.,* Numerical Investigation of the Steady Flamelet Approach under Different Combustion Environments, *Fuel*, *140* (2015), 1, pp. 731-743
[39] Yin, C., *et al*., Chemistry and Radiation in Oxy-Fuel Combustion: A Computational Fluid Dynamics Modeling Study, *Fuel*, *90* (2011), 7, pp. 2519-2529
[40] Guo, J., *et al.,* Numerical Investigation on Oxy-Combustion Characteristics of a 200 MWe Tangentially Fired Boiler, *Fuel*, *140* (2015), 1, pp. 660-668
[41] Field, M. A., *et al*., *Combustion of Pulverised Coal*, The British Coal Utilisation Research Association, Leatherhead, UK, 1967
[42] De Soete, G., Overall Reaction Rates of NO and N_2 Formation from Fuel Nitrogen, *Symposium (International) on Combustion*, *15* (1975), 1, pp. 1093-1102
[43] ***, IFRF Today, http://www.ffrc.fi/Liekkipaiva_2006/Liekkipaiva2006_IFRF_Today_HUPA.pdf
[44] Da Silva, R. C., *et al*., Flame Pattern, Temperatures and Stability Limits of Pulverized Oxy-Coal Combustion, *Fuel*, *115* (2014), 1, pp. 507-520
[45] Spliethoff, H., *Power Generation from Solid Fuels*, Springer, Berlin, 2010

Paper submitted: November 10, 2016
Paper revised: December 20, 2016
Paper accepted: December 22, 2016